Hybridization of antisense oligonucleotides with yeast tRNA^{Phe}: factors determining the efficiency of interaction

R. N. Serikov,[a,b] V. A. Petyuk,[a,b] V. V. Vlassov,[a] and M. A. Zenkova[a]★

[a]*Novosibirsk Institute of Bioorganic Chemistry, Siberian Branch of the Russian Academy of Sciences, 8 prosp. Akad. Lavrent´eva, 630090 Novosibirsk, Russian Federation, Fax: +7 (383 2) 33 3677. E-mail: marzen@niboch.nsc.ru*

[b]*Novosibirsk State University, 2 ul. Pirogova, 630090 Novosibirsk, Russian Federation.*

With the object of elucidating the factors that affect the rate and efficiency of oligonucleotide hybridization with complementary regions in natural RNA, the interaction of tRNA^{Phe} and *in vitro* transcript of this tRNA with synthetic oligonucleotides matching the 32—61 region comprising the variable loop and anticodon and TΨC stems of the molecule was studied in detail. Gel retardation was used to assay thermodynamic and kinetic parameters of tRNA interaction with oligonucleotides. Oligonucleotide hybridization rates do not depend on the oligonucleotide length and are determined by the stability of RNA structure within the binding site. The rate constant for hybridization correlates with the number of base pairs in the RNA opened during binding with the oligonucleotide. Factors stabilizing the tRNA secondary structure (the presence of Mg^{2+} ions, low temperature, hypermodified bases) decrease significantly both the rate and efficiency of hybridization. Analysis of the tRNA^{Phe} structure in the presence of an oligonucleotide shows that binding of oligonucleotides with the 45—61 region of tRNA^{Phe} results only in unfolding of the TΨC hairpin and does not disturb the secondary structure of the rest of the molecule.

Key words: tRNA^{Phe}, antisense oligonucleotides, hybridization, RNA structure.

The design of specific ligands that interact with nucleic acids is needed for investigations of the structure and functions of nucleic acids and for the development of gene-directed therapeutics affecting the expression of specific genes. By now, the most promising results in the targeted impact on RNA have been obtained by using oligonucleotide derivatives complementary to accessible nonstructured polynucleotide sequences.[1,2] Under physiological conditions, open, single-stranded nucleotide sequences in natural RNA are virtually missing, the real RNA targets represent a three-dimensional fold of certain nucleotide sequences.[3,4] Folding of single-stranded nucleic acids into a three-dimensional structure is a crucial factor hampering the interaction of antisense oligonucleotides with these biopolymers.[5] Further progress along this line is impossible without investigation of the factors affecting the efficiency of oligonucleotide interaction with elements of the secondary structure of natural nucleic acids.

Previously, it has been shown that oligodeoxyribonucleotides* can efficiently invade the structures of natural RNA [6] and even the stable structure of tRNAs.[7—10] It was found that, under nearly physiological conditions but in the absence of magnesium ions, oligonucleotides matching the 62—76 and 44—61 sequences of yeast tRNA^{Phe} were able to hybridize with this tRNA^{Phe} with association constants of about 10^4—10^5 L mol^{-1}.[10—12] We performed a detailed study of the interaction of oligonucleotides with yeast tRNA^{Phe} and elucidated the factors affecting the rate of oligonucleotide hybridization with natural RNA. The results obtained suggest unambiguously that the rate of oligonucleotide hybridization is determined by the stability of the RNA structure in the binding site and that the natural modified nucleobases also play a role in the structure stabilization.

* Below referred to as oligonucleotides for short.

Experimental

Commercial (Sigma) ribonucleoside triphosphates and deoxyribonucleoside triphosphates, acrylamide, *N*,*N*´-methylenebisacrylamide, $LiClO_4$, dithiothreitol (DTT), dithioerythritol (DTE), diethyl pyrocarbonate (DEPC), and "Stains-all", and Tris from Merck (Germany) were used. Other compounds were "high-purity," "reagent," or "analytical grade" commercial chemicals.

5´-[^{32}P]-Cytidine 3´,5´-bisphosphate (5´-[^{32}P]pCp) with a specific activity of ~4000 Ci mmol^{-1} produced by Biosan (Russia); T4 RNA-ligase produced by Fermentas (Lithuania), and

Published in Russian in *Izvestiya Akademii Nauk. Seriya Khimicheskaya,* No. 7, pp. 1067—1076, July, 2002.

1066-5285/02/5107-1156 $27.00

RNase ONE of Promega (USA) were used. The yeast $tRNA^{Phe}$ was a generous gift of Dr G. Kait (Institute de Biologie Moleculaire et Cellulaire du C.N.R.S., France). T7 RNA polymerase was prepared by V. N. Ankilova (Laboratory of Enzyme Biochemistry of the Novosibirsk Institute of Bioorganic Chemistry).

Oligonucleotides were synthesised at the Novosibirsk Institute of Bioorganic Chemistry by the standard phosphoramidite method and isolated using ion-exchange and reversed-phase HPLC.

All buffer solutions and reaction mixtures were prepared using MilliQ purified water (Millipore). The buffers were sterilized by filtration through a 0.22 μm nitrocellulose (Millipore).

The optical density was measured on an SF-46 spectrophotometer (Research and Production Concern LOMO, St. Petersburg). Polyacrylamide gels (PAAG) were dried *in vacuo* using a LABCONCO gel dryer. pH was measured on an Orion 410A pH-meter. Radioactivity was counted using a Canberra Packard counter. The gels were autoradiographed using a RENEKS X-ray film (Russia).

Preparation of the *in vitro* transcript of yeast $tRNA^{Phe}$. RNA was synthesized as described previously[13] using linearized plasmid p65YF0[14] containing a sequence of yeast $tRNA^{Phe}$ as a DNA template, under control of promoter of T7 phage RNA polymerase. The reaction mixture (1 mL) contained 40 *mM* Tris-HCl, pH 7.5, 6 *mM* $MgCl_2$, 2 *mM* spermidine, 10 *mM* NaCl, 10 *mM* DTT, 5 *mM* of each of ribonucleoside triphosphates (ATP, UTP, CTP, GTP), 50 μg of linearized plasmid, and 200 U of T7 phage RNA polymerase. The reaction mixture was incubated for 2 h at 37 °C. The incubation was followed by two successive extractions with equal volumes of water-saturated phenol and chloroform. Then RNA was precipitated with ethanol and kept for ~16 h at −20 °C, centrifuged (15 min, 4 °C, 14000 rpm), washed with ethanol, dried at 37 °C for 30 min, dissolved in 100 μL of an application solution (8 *M* urea containing 0.025% Bromophenol Blue and 0.035% Xylene Cyanole; solution 1), and applied onto 12% denaturing PAAG. The RNA band was visualized by UV shadow (λ 254 nm) using an intensifying screen (Merck). RNA was eluted from the gel by two 5-mL portions of the RNA elution buffer (0.3 *M* sodium acetate, pH 5.5, 10% phenol) for 18 h at 4 °C. A fourfold volume of ethanol was added to the eluted RNA, and the mixture was kept for ~16 h at −20 °C. The RNA pellet was recovered by centrifugation (15 min, 4 °C, 14000 rpm), washed with ethanol, dried at 37 °C for 30 min, and dissolved in water. The concentration of the *in vitro* $tRNA^{Phe}$ transcript was determined from the optical density at 260 nm. The yield of transcript after purification was 500—600 μg.

3′-[^{32}P]-Labeling to the tRNA. The introduction of the ^{32}P-label at the 3′-end of tRNA was carried out using a known method.[15] The standard 15-μL reaction mixture contained 0.1 OU_{260} individual $tRNA^{Phe}$, 50 *mM* HEPES-KOH, pH 7.5, 10 *mM* $MgCl_2$, 2 *mM* DTT, 10% DMSO, 100 μg mL^{-1} of bovine serum albumin, 20 mBq 5′-[^{32}P]-pCp and 20 U of T4 RNA ligase. To decrease the nonspecific degradation of tRNA during the enzymatic reaction, incubation with the enzyme was carried out at 4 °C for 18 h. After incubation, an equal volume of 8 *M* urea was added to the reaction mixture and the mixture was applied on the denaturing 10% PAAG. After electrophoresis, the gel was autoradiographed on a RENEKS film for 30 s. The tRNA band was cut out and eluted 3 times with 300 μL of 0.3 *M* sodium acetate, pH 5.5. tRNA was precipitated with ethanol at −20 °C for ~16 h. The tRNA precipitate was recovered by centrifugation (13000 rpm^{-1}, 15 min, 4 °C), washed with ethanol, dried, and dissolved in water, and the concentration and specific activity were determined. The typical specific activity of tRNA preparations was $(1—3)\cdot 10^5$ pulses $(min\ nmol)^{-1}$.

Dependence of the equilibrium binding extent on the oligonucleotide concentration. The oligonucleotide hybridization with $tRNA^{Phe}$ was assayed using the gel retardation technique.[16] Prior to hybridization, 3′-[^{32}P]-tRNA (final concentration in the mixture, 0.5 μmol L^{-1}) was incubated in water successively at 90 °C (1 min), 0 °C (1 min), and 20 °C (or 37 °C) for 10 min. After the addition of 2 μL of a buffer containing 250 *mM* HEPES-KOH, pH 7.5, 1 *M* KCl, and 0.5 *mM* EDTA or a similar buffer containing additionally 25 *mM* $MgCl_2$ to the aqueous solution of tRNA, the specimens were again incubated for 20 min at 20 °C (37 °C). The oligonucleotide in a concentration ranging from 0 to 1 *mM* was added to the tRNA mixture. After incubation for 6 h at 20 °C or for 1 h at 37 °C, 10-μL samples were mixed with 8 μL of the loading buffer (50% glycerol, 0.025% Bromophenol Blue, 0.025% Xylene Cyanole) equilibrated at 4 °C and applied immediately onto running 10% native PAAG. Electrophoresis was carried out in a 100 *mM* Tris-borate buffer (pH 8.3) for 6 h at 4 °C and at a voltage of 20 $V\,cm^{-1}$. After electrophoresis, the gel was dried and autoradiographed, the bands corresponding to the free tRNA and its complex with the oligonucleotide were cut out of the gel and the Cherenkov radiation was measured.

The experimental data were processed on an IBM PC computer using Excel 97 and Origin 5.0 softwares. The equilibrium binding constants were determined by optimization of the parameter K_A of Eq. (1), which relates the experimental degree of binding to the oligonucleotide concentration. The binding constant K_A was calculated by minimizing the mean-square deviation between the experimental curve and the theoretical curve derived from Eq. (1).

$$\alpha([X]) = K_A[X]/(1 + K_A[X]), \qquad (1)$$

where K_A is the equilibrium constant for oligonucleotide binding to $tRNA^{Phe}$; α([X]) is the degree of binding; [X] is the oligonucleotide concentration.

Kinetics of the oligonucleotide binding to $tRNA^{Phe}$. The samples were prepared as described above. The volume of the reaction mixture was 100 μL, the final tRNA concentration was 0.5 μmol L^{-1}, that of oligonucleotide was 20 μmol L^{-1}. At a specified moment, a 5-μL aliquot was taken from the reaction mixture, mixed with 5 μL of the loading buffer, and applied onto running native 10% PAAG. Electrophoresis and gel analysis were carried out as described in the previous section.

The rate constants for binding were determined by optimizing the parameters k_+ and k_- of Eq. (2), which relates the experimental degrees of binding (α) to time (t). The forward and reverse rate constants for hybridization were calculated by minimizing the mean-square deviations between the experimental curve and the theoretical curve based on Eq. (2).

$$\alpha(t) = k_+[X]/(k_+[X] + k_-)\cdot(1 - e^{-t(k+[X] + k-)}), \qquad (2)$$

where k_+, k_- are the rate constants for the forward and reverse reactions of oligonucleotide hybridization with $tRNA^{Phe}$.

Table 1. Sequences and binding sites of oligonucleotides 2A—2H and 2Z in the $tRNA^{Phe}$ structure

Oligonucleotide	Sequence	Length	Binding site
2A	GGATCGAACACAGGACCT	18	44—61
2B	GATCGAACACAGGACCT	17	44—60
2C	ATCGAACACAGGACCT	16	44—59
2D	TCGAACACAGGACCT	15	44—58
2E	GGATCGAACACAGGACC	17	45—61
2F	GGATCGAACACAGGAC	16	46—61
2G	GGATCGAACACAGGA	15	47—61
2H	GGATCGAA*ATACT*GACCT*	18	44—61
2Z	GACCTCCAGATCTTCA	16	32—49

* An oligonucleotide mismatch to the tRNA sequence is marked.

In some cases, when the curves did not reach a plateau, the rate constant for the forward hybridization reaction was determined from the slope ratio of the initial section of the kinetic curve.

Probing of the $tRNA^{Phe}$ structure in the course of hybridization with oligonucleotide 2C. Probing of tRNA was carried out using ribonuclease ONE.[17] The hybridization of 3′-[^{32}P]-$tRNA^{Phe}$ with oligonucleotide 2C (Table 1) was carried out as described above. A solution of RNase ONE (0.1 U, 1 μL) was immediately added to aliquots withdrawn from the reaction mixture (10 μL) at definite time intervals, and the mixture was incubated for 2.5 min at 20 °C. The hydrolysis was quenched by precipitating the RNA from the reaction mixture by a 2% solution of $LiClO_4$ in acetone. The mixtures were processed on a CENTRICON T-42K centrifuge (13 min, 13000 rpm) and the RNA pellets were dried, dissolved in loading buffer 1, and analyzed by electrophoresis in 12% PAAG under denaturing conditions. To identify the cleavage sites, partial hydrolyzates of RNA obtained using T1 RNase or under alkaline conditions were used as markers in RNA probing.[17]

Fluorescent titration. Pyrene derivatives of oligonucleotides were synthesized by a previously published procedure.[18] Fluorescence was measured on a Hitachi MPF4 fluorimeter with an excitation wavelength of 340 nm and an emission wavelength of 395 nm. Prior to hybridization, a solution of $tRNA^{Phe}$ with a concentration of 200 μmol L^{-1} was prepared in an HB buffer (50 *mM* HEPES-KOH, pH 7.5, 200 *mM* KCl, 0.1 *mM* EDTA) and a solution of modified oligonucleotide 5′-pyrenyl-2C was prepared in the same buffer with a concentration of 1.05 μmol L^{-1}. An oligonucleotide solution (190 μL) and an RNA solution (10 μL) were mixed in a 200-μL quartz cell maintained at 20 °C. The final concentrations of tRNA and the pyrene derivative of oligonucleotide 2C were 10 and 1 μmol L^{-1}, respectively. Immediately after mixing, fluorescence was measured; the intervals between the measurements were 30 s. The binding rate constants were determined by optimizing the k_+, k_- parameters of Eq. (3), which relates the experimental relative fluorescence values (f) to time (t). The forward (k_+) and reverse (k_-) rate constants for oligonucleotide hybridization with $tRNA^{Phe}$ were calculated by minimizing the mean-square deviation of the experimental curve from the theoretical curve plotted based on Eq. (3).

$$f(t) = a_1(k_+[X]/(k_+[X] + k_-)\cdot(1 - e^{-t(k_+[X] + k_-)}) + a_0, \quad (3)$$

where a_1 and a_2 are time-independent coefficients; $f(t)$ is the relative fluorescence; t is time; [X] is the RNA concentration.

Results and Discussion

Equilibrium hybridization of oligonucleotides with $tRNA^{Phe}$. Yeast $tRNA^{Phe}$ is one of the few RNA molecules whose secondary and tertiary structures have been studied in detail.[19,20] The tRNA secondary structure, the so-called clover leaf, consists of elements typical of most RNA, namely, D, TΨC, and anticodon hairpins, double-stranded regions, and an ACCA sequence at the 3′-end (Fig. 1). To study the interaction of oligonucleotides with RNA, we synthesized nine oligonucleotides of 2* series matching the $tRNA^{Phe}$ anticodon loop, variable loop, and TΨC loop regions (see Table 1, Fig. 1), which can be divided into four groups. The first group comprises oligonucleotides 2A, 2B, 2C, and 2D differing in length at the 5′-end in the part matching the TΨC loop. The second-group oligonucleotides (2A, 2E, 2F, and 2G) differ in length at the 3′-end in the part matching the variable loop. Oligonucleotide 2A is the reference oligonucleotide in all groups. The third group includes oligonucleotide 2H, an analog of 2A, which contains a sequence of five mismatches to the TΨC stem. Oligonucleotide 2Z is complementary to the anticodon hairpin and to the variable loop.

Hybridization of oligonucleotides with $tRNA^{Phe}$ was studied by gel retardation technique based on the difference between the electrophoretic mobilities of free and oligonucleotide-bound tRNA in 10% native PAAG. Binding of oligonucleotides 2A—2H and 2Z to $tRNA^{Phe}$

* Oligonucleotides of series 1 have been studied previously.[11,12]

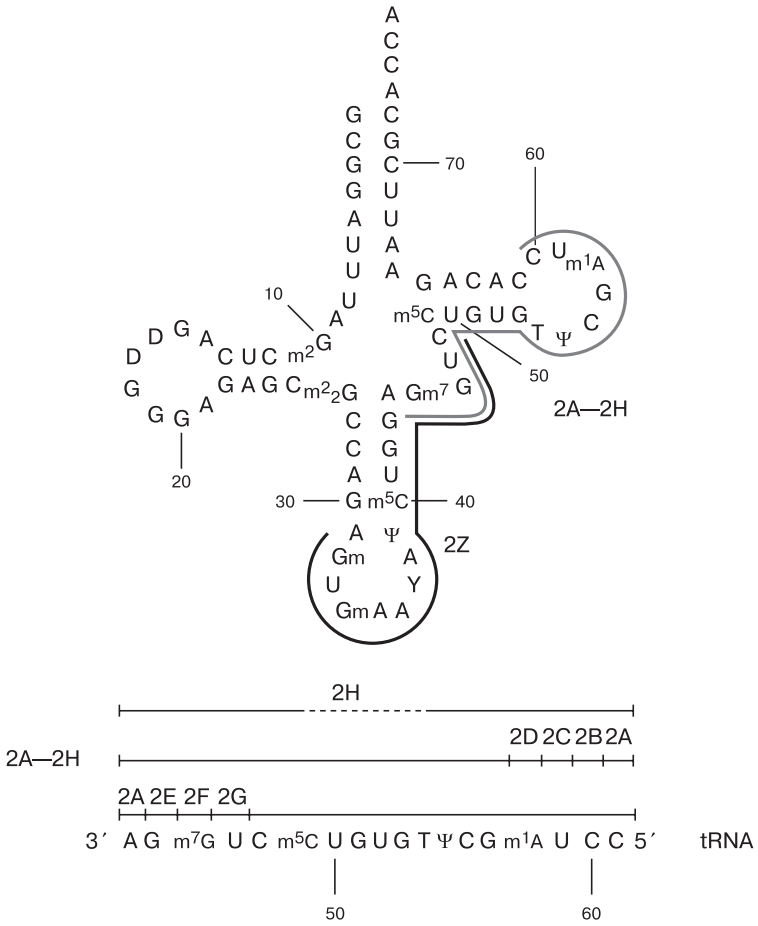

Fig. 1. Secondary structure of the yeast $tRNA^{Phe}$. The lines show oligonucleotide matching sequences. The dashed line shows the mismatches for oligonucleotide 2H.

was performed at an oligonucleotide concentration of 20 μmol L^{-1}, allowing the oligonucleotides to be differentiated according to the binding extent. A typical autoradiograph of a 10% native gel after separation of

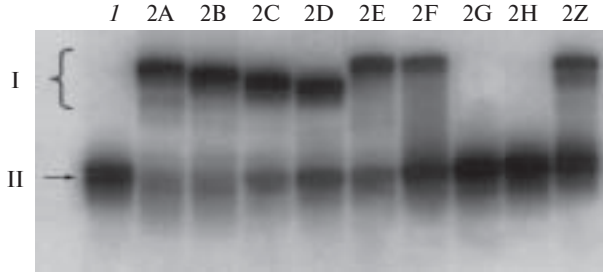

Fig. 2. Analysis of binding of oligonucleotides 2A—2H and 2Z to yeast $tRNA^{Phe}$ by the gel retardation method, (*I*) initial tRNA, I are complexes, II are $tRNA^{Phe}$. Autoradiograph of 10% native PAAG. The reaction mixtures containing $tRNA^{Phe}$ in a concentration of 0.5 μmol L^{-1}, oligonucleotides in a concentration of 20 μmol L^{-1}, 50 *mM* HEPES-KOH pH 7.5, 200 *mM* KCl, and 0.1 *mM* EDTA, were incubated at 20 °C for 6 h and applied on 10% native PAAG.

tRNA/oligonucleotide hybridization products is presented in Fig. 2. The quantitative data on the hybridization are given in Fig. 3, *a*. It can be seen from Figs 2 and 3, *a* that shortening of oligonucleotides from the side matching the 3′-part of the TΨC loop (first-group oligonucleotides) does not affect substantially the binding extent. Meanwhile, shortening of oligonucleotides in the region matching the variable loop (second-group oligonucleotides) results in a sharp drop of the binding extent from nearly 100% for oligonucleotide 2A to 0% for oligonucleotide 2G. These data suggest that a region of the variable loop representing a single-stranded sequence of five nucleotides is the most important for the oligonucleotide interaction with tRNA. Similar data were obtained in other studies,[11,12] in which efficient hybridization of oligonucleotides with the 68—76 3′-region of $tRNA^{Phe}$ was shown to require that they match the single-stranded ACCA sequence at the tRNA 3′-end. In addition, oligonucleotide 2H, which contains a mismatch to the TΨC stem, does not bind noticeably to the tRNA at any concentrations of the oligonucleotide. This indicates unambiguously that the 5′-fragment of the TΨC stem (nucle-

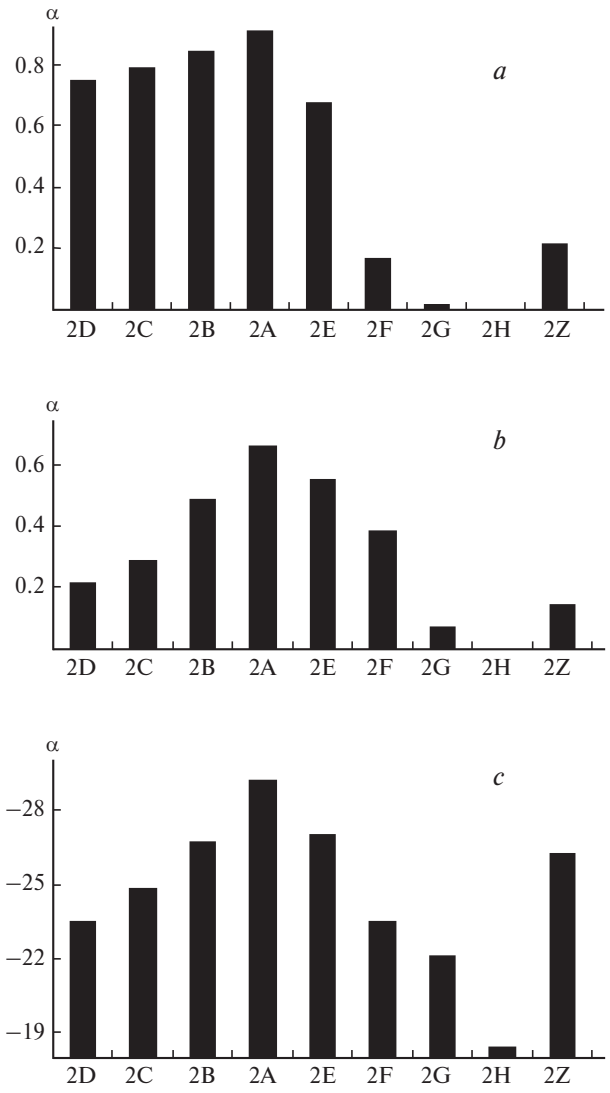

Fig. 3. Hybridization of oligonucleotides 2A—2H and 2Z with yeast $tRNA^{Phe}$.
a. Binding extent (α) of oligonucleotides to yeast $tRNA^{Phe}$ determined by the gel retardation method (the tRNA concentration is 0.5 μmol L^{-1}, the oligonucleotide concentration is 20 μmol L^{-1}).
b. Binding extent (α) of oligonucleotides with the *in vitro* transcript of yeast $tRNA^{Phe}$ determined by the gel retardation method (the tRNA concentration is 0.5 μmol L^{-1}, oligonucleotide concentration is 2 μmol L^{-1}).
c. Stability of oligonucleotide heteroduplexes with nonstructured complements calculated by the nearest neighbors method.[21]

otides 49—53) is involved in the interaction. The degree of binding of oligonucleotide 2Z matching the anticodon hairpin and the variable loop was ~20% for an oligonucleotide concentration of 20 μmol L^{-1}, which proves the possibility of oligonucleotide hybridization with one of the most stable natural hairpins (Fig. 3, *a*).

The matching region to oligonucleotides 2A—2H and 2Z contains a number of minor bases (m^1A, Ψ, m^7G, m^5C, Y), which can influence the efficiency of oligonucleotide hybridization with this tRNA region. To estimate the effect of minor bases on the oligonucleotide affinity for tRNA, hybridization of oligonucleotides 2A—2H, 2Z with the *in vitro* transcript of yeast $tRNA^{Phe}$ was studied. For each of oligonucleotides 2A—2H and 2Z in a concentration of 20 μmol L^{-1}, quantitative complex formation with the tRNA was observed. Comparison of the hybridization efficiency was performed for an oligonucleotide concentration of 2 μmol L^{-1} (Fig. 3, *b*). The character of binding of oligonucleotides 2A—2H and 2Z to the *in vitro* transcript of yeast $tRNA^{Phe}$ (see Fig. 3, *a*) differs basically from that to the mature $tRNA^{Phe}$ (see Fig. 3, *b*). Stepwise shortening of oligonucleotides from both 3′- and 5′-ends results in a gradual decrease in the degree of binding, which correlates with the stability of heteroduplexes (Fig. 3, *c*) formed by oligonucleotides 2A—2H and 2Z with the linear strands calculated by the nearest neighbors method.[22] However, in the case of the *in vitro* $tRNA^{Phe}$ transcript, too, shortening of oligonucleotides from the 3′-end (2A, 2E, 2F, and 2G) still entails a sharper decrease in the binding efficiency than shortening from the 5′-end.

Hybridization of tRNA with each of the oligonucleotides in the concentration range from 1.75 to 840 μmol L^{-1} at 20 °C (Table 2) was carried out to determine the equilibrium binding constants (K_x). Reliable determination of the constants was possible only for those oligonucleotides whose binding extent was at least 50%. It can be seen from Table 2 that hybridization of oligonucleotide 2Z with anticodon hairpin decreases

Table 2. Influence of magnesium ions, temperature, and minor bases on the equilibrium and kinetic constants[a] of oligonucleotide hybridization with yeast $tRNA^{Phe}$

Oligonucleotide	T /°C	5 *mM* Mg^{2+}	k_+^{eff} [b] /L mol^{-1} s^{-1}	K_A [c] /L mol^{-1}
2A	20	—	5.23±0.46	$(9.2\pm0.3)\cdot10^5$
	20	+	$(2.01\pm0.09)\cdot10^{-1}$	
2C	20	—	5.81±0.18	$(7.7\pm0.5)\cdot10^5$
	37	+	8.15±0.58	
2Z	20	—	3.85±0.23	$(2.2\pm0.5)\cdot10^4$
	37	+	1.03±0.17	

[a] The efficiency of oligonucleotide hybridization with yeast $tRNA^{Phe}$ was assayed by the gel retardation method for tRNA concentration of 0.5 μmol L^{-1} and oligonucleotide concentration of 20 μmol L^{-1}.
[b] The rate constant for hybridization was calculated by minimizing the mean-square deviations between the experimental curve and the theoretical curve based on Eq. (2).
[c] Association constant K_A was calculated by minimizing the mean-square deviations between the experimental curve and the theoretical curve based on (1).

the equilibrium constant by a factor of 30 (oligonucleotides 2C and 2Z).

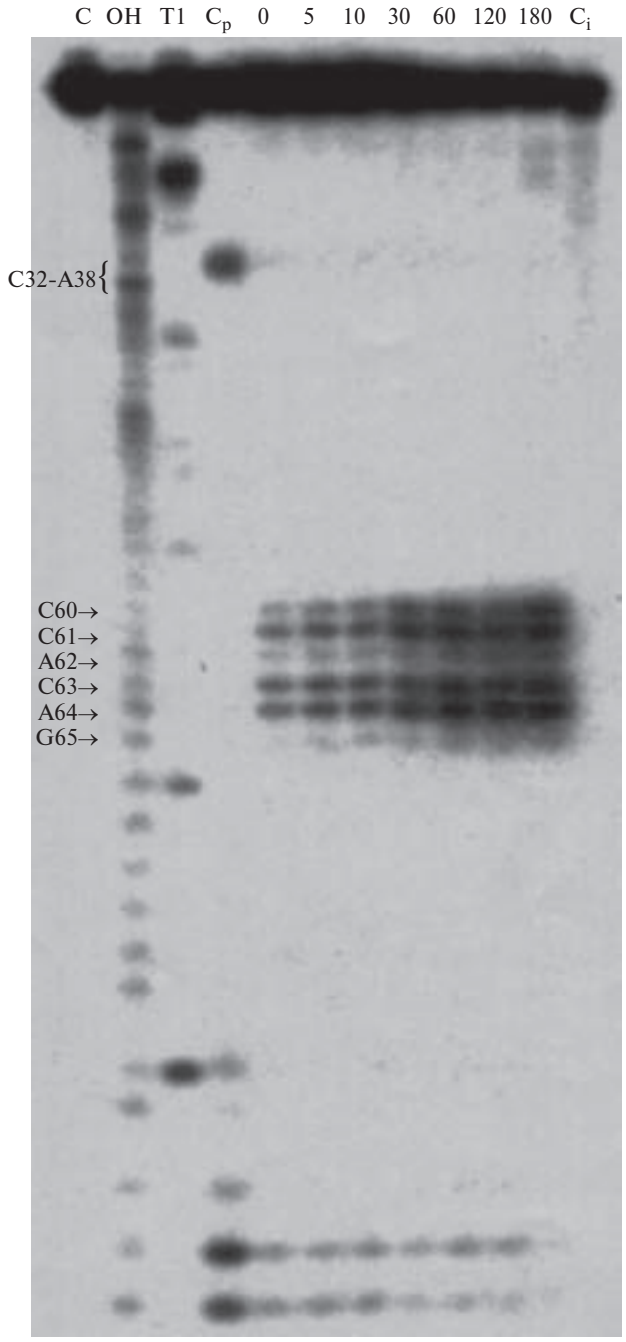

Fig. 4. Probing of the $tRNA^{Phe}$ structure in the complex with oligonucleotide 2C. Autoradiograph of denaturing 12% PAAG after separation of the 3′-[^{32}P]-$tRNA^{Phe}$ hydrolyzate during hybridization with the oligonucleotide. Lanes: C is the initial tRNA; OH, T1 are tRNA partial hydrolyzates by alkali and by T1 RNase under denaturing conditions; C_p is tRNA hydrolyzed by RNase ONE in the absence of oligonucleotide; lanes 0, 5, 10, 30, 60, 120, and 180 correspond to the time of $tRNA^{Phe}$ incubation with the oligonucleotide (0, 5, 10, 30, 60, 120, and 180 min); C_i is the incubation control of tRNA.

Probing of the tRNA structure in the course of hybridization with oligonucleotides. Changes in the $tRNA^{Phe}$ structure upon binding to oligonucleotide 2C were studied using probing of RNA within a heteroduplex with oligonucleotide 2C by RNase ONE. This enzyme was used because RNase ONE is active under hybridization conditions and the time of limited hydrolysis by this enzyme (2.5 min) is much shorter than the hybridization half-period ($\tau_{1/2}$ ~1 h). Samples of the 3′-^{32}P-labeled tRNA were incubated with oligonucleotide 2C for defined time intervals (0 → 180 min) and then subjected to partial hydrolysis by RNase ONE (Fig. 4). The results of probing show that the hybridization site of oligonucleotide 2C coincides with the matching sequence and that only one complex is formed. The formation of the 2C • $tRNA^{Phe}$ heteroduplex causes unfolding of the TΨC stem of tRNA and barely influences the 3D structure of other tRNA elements.

Two stages, fast and slow, can be distinguished during hybridization. Immediately after the addition of oligonucleotide 2C, RNA hydrolysis in the regions of the ACCA end and the anticodon loop (region 32—38) is inhibited. Fast inhibition of hydrolysis is apparently due to the formation of partially matching complexes with these RNA regions. Slow processes detectable by the probing occur in the vicinity of the TΨC stem. It should be noted that oligonucleotide 2C hybridization with $tRNA^{Phe}$ does not result in any global rearrangement of the $tRNA^{Phe}$ structure, which has been observed for oligonucleotide 1D.[12]

Kinetics of oligonucleotide hybridization with yeast $tRNA^{Phe}$. The kinetics of oligonucleotide binding to the natural $tRNA^{Phe}$ was assayed by gel retardation technique for fixed concentrations of oligonucleotides (20 μmol L^{-1}) and $tRNA^{Phe}$ (0.5 μmol L^{-1}). The reaction was carried out under various conditions: at 20 or 37 °C and in the presence or absence of magnesium ions. Study of the hybridization kinetics was reliable only for those oligonucleotides whose equilibrium degree of binding under the given conditions was no less than 50%. Typical kinetics of oligonucleotide hybridization with tRNA is shown in Fig. 5, *a*. The variations of the degrees of oligonucleotide binding to tRNA *vs.* time for a number of oligonucleotides are presented in Fig. 5, *b* (for comparison, data for oligonucleotide 1D are given[12]). At 20 °C, hybridization of oligonucleotides with tRNA proceeds slowly, the half-reaction period being 0.5 h. This rather low rate is due apparently to the rigidity of the $tRNA^{Phe}$ structure at 20 °C. If excess oligonucleotide (ON) is present in the reaction mixture ([2C] = 20 μmol L^{-1}, [tRNA] = 0.5 μmol L^{-1}), quasi-linear assumptions may be applied and, in analyzing the quantitative data obtained, the oligonucleotide concentration may be considered constant. In this case, the kinetic

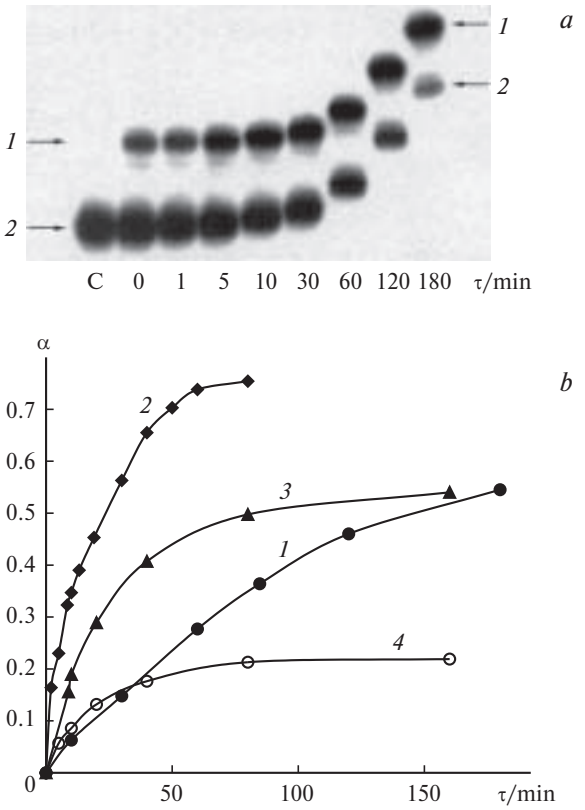

Fig. 5. Kinetics of oligonucleotide 2C hybridization with $tRNA^{Phe}$ at 20 °C.
a. Autoradiograph of the native 10% PAAG after separation of free tRNA from that bound to oligonucleotide 2C ([$tRNA^{Phe}$] 0.5 μmol L^{-1} and [2C] 20 μmol L^{-1}, a standard hybridization buffer): *1*, tRNA·ON complex; *2*, tRNA; C, the starting tRNA (lanes 0, 1, 5, 10, 30, 60, 120, 180 correspond to the incubation time of 0, 1, 5, 10, 30, 60, 120, 180 min respectively).
b. Kinetic curves for binding of oligonucleotides 1D (*1*), 2A (*2*), 2C (*3*), and 2Z (*4*) to yeast $tRNA^{Phe}$ at 20 °C ([tRNA] = $5 \cdot 10^{-7}$ mol L^{-1}, [ON] = $2 \cdot 10^{-5}$ mol L^{-1}).

curves for the hybridization are described by reaction (4) and Eq. (5):

$$\text{tRNA} + \text{ON} \underset{k_-}{\overset{k_+}{\rightleftharpoons}} \text{tRNA}\cdot\text{ON}, \qquad (4)$$

$$a(t) = (k_+^{\text{eff}}/(k_+^{\text{eff}} + k_-)\cdot(1 - e^{-t(k+\text{eff} + k-)}), \qquad (5)$$

where $k_+^{\text{eff}} = k_+[X]$.

The rate constants for oligonucleotides hybridization thus found are listed in Table 2. The data on the kinetics of oligonucleotide binding to tRNA were obtained by averaging the data of two independent experiments. The rate constants are very low (3—5 L mol^{-1} s^{-1}) compared to the known rate constants for the formation of duplexes between two linear oligonucleotides (k_+ = 10^5—10^6 L mol^{-1} s^{-1} (21—23 °C)[23]) or hybridization of two structured RNA (k_+ = 10^3—10^4 L mol^{-1} s^{-1} (37 °C)[24]). No correlation between the rate constants for oligonucleotide hybridization and the oligonucleotide length or, correspondingly, the stability of the heteroduplex formed was found. In general, both k_+ and k_- values for oligonucleotides 2A, 2C, and 2Z lie within very narrow limits.

Using oligonucleotide 2C as an example, the kinetics of complexation determined by the gel retardation method was compared with the results obtained by fluorescence quenching. Hybridization of the 5′-pyrenyl derivative of oligonucleotide 2C with $tRNA^{Phe}$ causes quenching of the pyrene fluorescence (Fig. 6). The value $\tau_{1/2} \approx 15$ min found by fluorescence quenching ([$tRNA^{Phe}$] = 10 μmol L^{-1}, [2C] = 1 μmol L^{-1}) is comparable with the value $\tau_{1/2} \approx 35$ min determined by the gel retardation method for the reaction of oligonucleotide 2C derivative with a mature $tRNA^{Phe}$ ([$tRNA^{Phe}$] = 0.5 μmol L^{-1}, [2C] = 20 μmol L^{-1}). In both cases, the process is slow. The difference between the half-reaction periods is due to the different hybridization conditions and reactant concentrations. Thus, it can be claimed

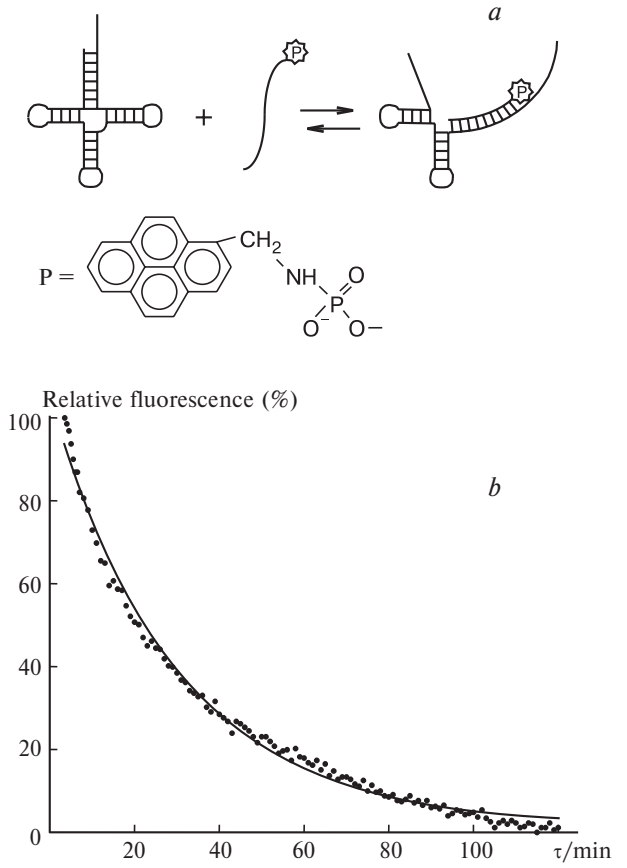

Fig. 6. *a*. Interaction of the oligonucleotide 2C pyrene derivative with the *in vitro* transcript of yeast $tRNA^{Phe}$. *b*. Fluorescence quenching upon binding of the pyrene derivative of oligonucleotide 2C to the *in vitro* transcript of yeast $tRNA^{Phe}$ at 20 °C ([tRNA] = 10^{-5} mol L^{-1}, [2C] = 10^{-6} mol L^{-1}).

that, generally, the gel retardation technique provides adequate quantitative data on the interaction of oligonucleotides with tRNA.

The conclusion concerning the key role of the RNA secondary structure in the hybridization is supported by the fact that the rate constant for hybridization depends on the factors affecting the stability of the tRNA structure, namely, the temperature, the addition of magnesium ions, and the presence of minor bases. We studied the influence of various factors on the rates of binding of oligonucleotides 2A, 2C, and 2Z to $tRNA^{Phe}$. The observed rate constants are listed in Table 2. It can be seen that the rates of oligonucleotide hybridization with the mature $tRNA^{Phe}$ and with the *in vitro* transcript of $tRNA^{Phe}$ containing no modified bases differ by a factor of 30. The addition of magnesium ions, which stabilize the 3D structure of tRNA, decreases the rate constants for the forward reactions of both the *in vitro* $tRNA^{Phe}$ transcript and the mature $tRNA^{Phe}$ (by factors of 50 and 100, respectively). An increase in the hybridization temperature from 20 to 37 °C induces a substantial increase in the rate constant for the forward reaction (approximately 150-fold without Mg^{2+} ions and 1000-fold in the presence of Mg^{2+} ions).

These results suggest that an efficient reaction with an oligonucleotide requires the presence of a short single-stranded sequence in the target RNA structure; it is possible to determine the size of this sequence. Oligonucleotides 2A, 2B, 2C, and 2D, which bind efficiently, match seven, six, five, and four bases located in the TΨC loop, respectively, and five more bases in the variable loop (Table 3). Oligonucleotides 2A, 2E, 2F, and 2G match five, four, three, and two bases, respectively, in this region. Oligonucleotide 2G, which is not hybridized with tRNA, matches seven bases of the TΨC loop (like 2A) and only two bases of the variable loop. Shortening of series 2 oligonucleotides in the region matching the variable loop (oligonucleotides 2A, 2E, 2F, 2G) entails a pronounced decrease in the efficiency of binding, whereas shortening of the oligonucleotide from the 5′-end does not induce such substantial changes. This might be due to the fact that even the shortest oligonucleotide 2D retains a section matching five bases of the TΨC loop in its sequence. Thus, the single-stranded section needed for efficient hybridization should not be smaller than three or four bases in size. The function of this RNA section is, apparently, to initiate the formation of a heteroduplex, similarly to the nucleation site in the duplex formation between linear oligonucleotides.[25] Unlike the nucleation site of linear oligonucleotides, whose size was determined to be two base pairs, an efficient nucleation in the formation of a heteroduplex between the oligonucleotide and a structured RNA requires a more extended single-stranded RNA sequence. It cannot be ruled out that in the interaction of oligonucleotide with the structured RNA, the size of the nucleation site remains the same as in the case of linear molecules, but invasion of the oligonucleotide into the RNA structure requires the formation of an intermediate complementary complex, three or four base pairs long.

For the formation of a stable oligonucleotide complex with tRNA, the energy of the heteroduplex formed should be lower than the energy of the structure of the RNA section being unfolded. Evidently, the greater the energy benefit, the higher the oligonucleotide affinity to the RNA target. Oligonucleotides of series 2 represent an apparent exception to this rule. Indeed, upon shortening of oligonucleotide 2A from the 5′-end (2A, 2B, 2C, 2D), a decrease in the hybridization capacity is hardly observed and does not correlate with the calculated sta-

Table 3. Effect of the length of the oligonucleotide binding site and the size of the single-stranded section on the efficiency of oligonucleotide hybridization with yeast $tRNA^{Phe}$

Oligonucleotide	Length	Single-stranded region		Degree of binding	
		TΨC loop	Variable loop	$tRNA^{Phe}$ [a]	$tRNA^{Phe}$ transcript [b]
2A	18	7	5	0.9	0.7
2E	17	7	4	0.7	0.55
2F	16	7	3	0.15	0.4
2G	15	7	2	0.01	0.1
2A	18	7	5	0.9	0.7
2B	17	6	5	0.85	0.5
2C	16	5	5	0.8	0.3
2D	15	4	5	0.75	0.2
1D	15		4[c]	0.8	—

[a] For tRNA concentration of 0.5 μmol L^{-1} and oligonucleotide concentration of 20 μmol L^{-1}.
[b] For tRNA concentration of 0.5 μmol L^{-1} and oligonucleotide concentration of 2 μmol L^{-1}.
[c] Hybridization with the single-stranded ACCA sequence at the 3′-end of tRNA.

Table 4. Dependence of the rate of oligonucleotide hybridization with $tRNA^{Phe}$ on the number of opened base pairs and hybridization section

Oligo-nucleotide	Rate constant /L mol^{-1} s^{-1}	The number of opened base pairs	Binding site
1D	1.9	12	Acceptor stem + TΨC hairpin
2C	5.8	5	TΨC hairpin
2Z	3.9	5	Anticodon hairpin

bilities of heteroduplexes. This can be explained only by assuming that the 5′-end bases of the oligonucleotide make no contribution to the stability of the heteroduplex formed. The tRNA region matching the 5′-end of oligonucleotides contains a minor base m^1A, which is unable to form a Watson-Crick pair, unlike other minor bases (T, Ψ, m^5C, m^7G) located in this section. Probably, the bases at the 5′-end of oligonucleotides 2A, 2B, 2C, and 2D form a "dangling" end and make no contribution to the energy of heteroduplex formation. This suggestion is confirmed by the data on hybridization of the same oligonucleotides with the *in vitro* transcript of $tRNA^{Phe}$.

In the case of the $tRNA^{Phe}$ transcript, the decrease in the affinity of oligonucleotides (2A, 2B, 2C, 2D) to the RNA target correlates with the calculated stabilities of heteroduplexes (see Fig. 3, *c*). Previously, effects of this type have been observed for the $tRNA^{Tyr}$ from *E. coli* [21] and for the bovine mitochondrial $tRNA^{Ser}(AGY)$.[8] In both cases, the decrease in the binding extent of oligonucleotides was due to the hypermodified bases located directly after the 3′-end nucleotide of the anticodon triplet, ms^2i^6A and t^6A. In the case of yeast $tRNA^{Phe}$, the hypermodified base in the 3′-pair of the anticodon loop is represented by weibutin (Y), which might decrease the efficiency of hybridization of oligonucleotide 2Z with tRNA.

At 20 °C, binding of oligonucleotides to the yeast $tRNA^{Phe}$ is slow. The rate of hybridization of oligonucleotides having the same nucleation site virtually does not depend on the length of the oligonucleotide (2A and 2C). This is possible, provided that unfolding of the tRNA structure in the section matching the oligonucleotide is the limiting step of the hybridization. The effective rate constants for binding for 16-mer oligonucleotides matching different sections are 1.84 [12] (1D), 5.81 (2C), and 3.85 (2Z) L mol^{-1} s^{-1} (Table 4). Hybridization of oligonucleotide 1D causes disruption of 12 base pairs, which is apparently responsible for the lowest binding rate constant. For each of oligonucleotides 2C and 2Z, five base pairs need to be disrupted in the tRNA. However, oligonucleotide 2C matches the TΨC hairpin and 2Z, the more stable anticodon hairpin,[26] which is reflected accordingly in the corresponding rate constants.

In the presence of 5 *mM* $MgCl_2$, the binding rate constant decreases 100-fold for oligonucleotide 2C and 25-fold for oligonucleotide 2A (at 20 °C). The yeast $tRNA^{Phe}$ has four sites for specific binding of magnesium ions,[27] which stabilize substantially the tRNA 3D structure, thus hampering oligonucleotide binding. In oligonucleotide 2C hybridization with the *in vitro* $tRNA^{Phe}$ transcript, the binding rate markedly increases (approximately 30-fold). This result is consistent with the published data indicating that minor bases stabilize the 3D structure of tRNA.[28] These data are also in line with the assumption concerning the crucial role of unfolding of the RNA structure during hybridization. An increase in the hybridization rate constant both in the presence and in the absence of magnesium ions is observed as the temperature rises from 20 to 37 °C. This is related to the general destabilization of the tRNA 3D structure at higher temperatures, which facilitates binding. This behavior of k_+ attests to a positive activation energy of the forward hybridization reaction. Similar conclusions have been drawn in investigations[29—31] of the hybridization kinetics of antisense RNA with their biological targets, natural RNA.

* * *

The kinetic aspects of the interactions of oligonucleotides matching various RNA structures still remain little studied. The results obtained in this work are useful for understanding the principles of interactions between antisense oligonucleotides and RNA. The results of our experiments indicate that the rate of oligonucleotide hybridization with RNA is determined exclusively by the stability of the RNA structure in the oligonucleotide binding site and does not depend on the oligonucleotide length. The factors that destabilize the 3D RNA structure (higher temperature, the absence of magnesium ions) increase both the rate and the equilibrium constant of hybridization. Conversely, the presence of magnesium ions decreases the rate and the equilibrium constant of oligonucleotide binding to RNA by destabilizing the RNA structure. The data on the equilibrium hybridization of oligonucleotides with tRNA permit one to conclude that efficient binding of oligonucleotides to natural RNA re-

quires the presence of open single-stranded sequences, three or four bases long, in the site matching the oligonucleotide; these are important for productive nucleation and for initiation of the formation of the heteroduplex.

This work was financially supported by the Russian Foundation for Basic Research (Projects No. 00-15-97969 and No. 01-04-49003), U. S. Civilian Research and Development Foundation (Grant REC-008), and the Siberian Branch of the Russian Academy of Sciences (Grant for Young Scientists and Grant for International Projects of the Siberian Branch of the Russian Academy of Sciences, No. 26).

References

1. S. T. Crooke, *Methods Enzymol.*, 2000, **313**, 3.
2. D. J. Ecker, in *Antisense research and applications*, Eds. S. T. Crooke and B. Lebleau, CRC Press, Boca Raton, 1993, 387.
3. S. Baskerville and A. D. Ellington, *Curr. Biol.*, 1995, **5**, 120.
4. R. T. Batey, R. P. Rambo, and J. A. Doudna, *Angew. Chem. Int., Ed. Engl.*, 1999, **38**, 2326.
5. A. D. Branch, *Trends Biochem. Sci.*, 1998, **23**, 45.
6. R. A. Stull, G. Zon, and F. C. Szoka, Jr., *Antisense Nucleic Acid Drug. Dev.*, 1996, **6(3)**, 221.
7. K. U. Mir and E. M. Southern, *Nature Biotechnol.*, 1999, **17**, 788.
8. Y. Kumazawa, T. Yokogawa, H. Tsurui, K. Miura, and K. Watanabe, *Nucleic Acids Res.*, 1992, **20**, 2223.
9. T. Kanda, K. Takai, S. Yokoyama, and H. Takaku, *Bioorg. Med. Chem.*, 2000, **8**, 675.
10. V. Petyuk, R. Serikov, V. Tolstikov, V. Potapov, R. Giege, M. Zenkova, and V. Vlassov, *Nucleosides, Nucleotides Nucleic Acids,* 2000, **19**, 1145.
11. V. Petuyk, M. Zenkova, R. Giege, and V. V. Vlassov, *FEBS Letters*, 1999, **444**, 217.
12. V. A. Petyuk, M. A. Zenkova, R. Giege, and V. V. Vlassov, *Molekulyar. Biol.*, 2000, **34**, 879 [*Mol. Biol.*, 2000, **34** (Engl. Transl.)].
13. J. F. Milligan and O. C. Uhlenbeck, *Methods Enzymol.*, 1989, **180**, 51.
14. J. R. Sampson and O. C. Uhlenbeck, *Proc. Natl. Acad. Sci. USA*, 1988, **85**, 1033.
15. T. E. England, A. G. Bruce, and O. C. Uhlenbeck, *Methods Enzymol.*, 1980, **65**, 65.
16. D. Lane, P. Prentki, and M. Chandler, *Microbiol. Rev.*, 1992, **56(4)**, 509.
17. J. Meador, B. Cannon, V. J. Cannistraro, and D. Kennell, *Eur. J. Biochem.*, 1990, **187**, 549.
18. M. I. Dobrikov, S. A. Gaidamakov, A. A. Koshkin, T. I. Guinutdinov, N. P. Luk´yanchuk, G. V. Shishkin, and V. V. Vlassov, *Bioorgan. Khim.*, 1997, **23**, 191 [*Russ. J. Bioorg. Chem.*, 1997, **23** (Engl. Transl.)].
19. M. Sprinzl, *Eur. J. Biochem.*, 1974, **49**, 595.
20. J. D. Robertus, J. E. Ladner, J. T. Finch, D. Rhodes, R. S. Brown, B. F. Clark, and A. Klug, *Nature*, 1974, **250**, 546.
21. O. C. Uhlenbeck, *J. Mol. Biol.*, 1972, **65**, 25.
22. N. Sugimoto, S. Nakano, M. Katoh, A. Matsumura, H. Nakamuta, T. Ohmichi, M. Yoneyama, and M. Sasaki, *Biochemistry*, 1995, **34**, 11211.
23. M. E. Craig, D. M. Crothers, P. Doty, *J. Mol. Biol.*, 1971, **62**, 383.
24. V. Patzel and G. Szakiel, *Nucleic Acids Res.*, 2000, **13**, 2462.
25. C. R. Cantor and P. R. Schimmel, in *Biophysical Chemistry, Part 3: The Behavior of Biological Macromolecules*, W. H. Freeman, San Francisco, 1980, **3**, 23.
26. O. Pongs and E. Reinwald, *Biochem. Biophys. Res. Commun.*, 1973, **50**, 357.
27. P. Narayan and F. Ramirez, *Biochim. Biophys. Acta*, 1978, **518**, 539.
28. P. F. Agris, A. Malkiewicz, R. Guenther, M. Basti, R. Sengupta, and J. Stuart, *Nucleic Acids Symp. Ser.*, 1995, **33**, 254.
29. M. Homann, K. Rittner, and G. Sczakiel, *J. Mol. Biol.*, 1993, **233**, 7.
30. K. Rittner, C. Burmester, and G. Sczakiel, *Nucleic Acids Res.*, 1993, **21**, 1381.
31. R. Kronenwett, R. Haas, and G. Sczakiel, *J. Mol. Biol.*, 1996, **259**, 632.

Received September 25, 2001;
in revised form December 24, 2001